



ORIGINAL ARTICLE

Polyethylene glycol functionalized $\text{Fe}_3\text{O}_4@\text{MIL-101}(\text{Cr})$ for the efficient removal of heavy metals from *Ligusticum chuanxiong* Hort



Qingrong Han^a, Fei Liu^b, Chengjiu Wang^a, Zhentao Tang^{c,*}, Cheng Peng^{a,*},
Yuzhu Tan^{a,*}

^a Key Laboratory of Southwestern Chinese Medicine Resources, School of Pharmacy, Chengdu University of Traditional Chinese Medicine, Chengdu, China

^b Technology Center of Chengdu Customs District P.R. China, Chengdu, China

^c Key Laboratory of Southwestern Chinese Medicine Resources, Innovative Institute of Chinese Medicine and Pharmacy, Chengdu University of Traditional Chinese Medicine, Chengdu, China

Received 3 September 2022; accepted 26 January 2023

Available online 1 February 2023

KEYWORDS

Ligusticum chuanxiong Hort;
Heavy metals;
Removal;
Magnetic nanomaterial;
MOFs;
Polyethylene glycol

Abstract In recent years, the quality and safety issues of Chinese medicinal herbs have received great attention worldwide. Thereinto, heavy metal contamination has been one of the most serious concerns. Compared to the wide research in the analysis of heavy metals in medicinal herbs, the studies on the removal of heavy metals are relatively limited. In this study, polyethylene glycol functionalized $\text{Fe}_3\text{O}_4@\text{MIL-101}(\text{Cr})$ ($\text{Fe}_3\text{O}_4@\text{MIL-101}(\text{Cr})@\text{PEG}$) was designed and synthesized to remove heavy metals from the decoction of *Ligusticum chuanxiong* Hort. The in-house fabricated $\text{Fe}_3\text{O}_4@\text{MIL-101}(\text{Cr})@\text{PEG}$ was characterized by a porous structure and a large specific surface area. Then, the efficiency of the material for the removal of five heavy metals was tested under optimal adsorption conditions. Meanwhile, the content of Senkyunolide A, Senkyunolide I, and Ferulic acid, the solid content, and the HPLC fingerprints similarity were used as the quality monitoring indicators of *Ligusticum chuanxiong* Hort decoction before and after the heavy metal removal. Results showed that the magnetic nanomaterial had excellent removal efficiency for As^{5+} (81.4 %), Cd^{2+} (88.19 %), and Pb^{2+} (83.79 %) and certain removal efficiency for Ni^{2+} (51.59 %) and Zn^{2+} (55.4 %) under the spiked concentration of 50 $\mu\text{g}/\text{mL}$. The content of Senkyunolide A, Senkyunolide I, and Ferulic acid were decreased by less than 8.00 % after the removal of heavy metals. Besides, the loss rate of solid content was only 0.18 %, and the finger-

* Corresponding authors.

E-mail addresses: zttang@cdutcm.edu.cn (Z. Tang), pc@cdutcm.edu.cn (C. Peng), tanyuzhu@cdutcm.edu.cn (Y. Tan).

Peer review under responsibility of King Saud University.



prints similarity was over 99.9 %. The results indicated that $\text{Fe}_3\text{O}_4@\text{MIL-101}(\text{Cr})@\text{PEG}$ could efficiently and selectively remove heavy metals from *Ligusticum chuanxiong* Hort without affecting its effective components. Due to the advantages of low-cost, simple manipulation, and good efficiency, the material can be recommended for heavy metals removal from the aqueous solutions of medicinal herbs, providing a new and promising application for the removal of exogenous contaminants in medicinal herbs.

© 2023 The Author(s). Published by Elsevier B.V. on behalf of King Saud University. This is an open access article under the CC BY-NC-ND license (<http://creativecommons.org/licenses/by-nc-nd/4.0/>).

1. Introduction

Heavy metals have toxic effects on the body's metabolism and normal physiological functions, some of which have been recognized as harmful trace elements to the human body, such as Pb, Cd, Hg, and As. Excessive consumption of heavy metals in the human body can lead to various diseases, such as renal failure, chronic toxic symptoms, liver injury, and even cancer (Azimi et al., 2017). As common extrinsic contaminants in medicinal herbs, heavy metals not only affect the quality and safety of medicinal herbs but also hinder the long-term development of the related industry (Yanhong et al., 2017). At present, the content of heavy metals has become one of the important indicators of controlling the quality and safety of medicinal herbs (Coghlan et al., 2015; Lin et al., 2018). The contamination during planting and processing causes the accumulation of heavy metals in some medicinal herbs, which even exceed the maximum residue limits (MRLs) (Xionghai & Yitong, 2004). Some research shows that the excessive content of heavy metals in Chinese medicinal materials is widespread (Liang & Liang, 2021). For example, the total over-limit ratio of heavy metals was 22 % in 100 commonly used traditional Chinese medicines (Feng et al., 2014). Thereinto, the over-limit ratio of Cd, Pb, As, and Hg was 19 %, 5 %, 2 %, and 1 %, respectively. According to the statistical analysis of the literature about heavy metals pollution in traditional Chinese medicine from 2000 to 2016, the over-limit ratio of Pb, As, Cd, and Hg in traditional Chinese medicine was 3.46 %, 4.03 %, 2.91 %, and 1.41 %, respectively (Guo et al., 2017). Therefore, the pollution of heavy metals in traditional Chinese medicine was still one of the serious problems regarding its quality and safety. Most of the studies presently focused on the detection of heavy metals in medicinal herbs (Zhang et al., 2021), while limited ones were about the removal of heavy metals. It is urgent to establish effective methods for the removal of heavy metals in medicinal herbs to improve the quality of traditional Chinese medicine and ensure its sustainable development.

Up to now, numerous techniques have been used to remove heavy metals from water and other matrices, such as chemical precipitation, adsorption, biosorption, ion exchange, coagulation-flocculation, membrane separation, and supercritical fluid extraction (Fu & Wang, 2011; Turhanen et al., 2015; Yang et al., 2019). Thereinto, adsorption is one of the most commonly used methods. In this way, different adsorbents have been developed and applied, including carbon-based nanomaterials, molecular imprinting polymers, chitosan, magnetic nanoparticles, metal-organic frameworks (MOFs), etc. MOFs, a new kind of crystalline porous material formed by metal ions/clusters and multidentate organic ligands, are emerging as an attractive class of adsorbents (Zhou et al., 2012). They are generally characterized by open frameworks with accessible channels and cage structures (Jalayeri et al., 2020; Xiaolei Zhang et al., 2020). Due to their extraordinary properties, represented by high surface area, porous structures, tunable pores, availability of in-pore and outer-surface functionalization, and excellent mechanical stability, MOFs show great potential for the adsorption of hazardous pollutants (Hasan et al., 2016; Shi et al., 2018; Wang et al., 2015). MIL-101(Cr) is a self-assembly of Cr^{3+} ions and an organic ligand (terephthalic acid). Compared with other MOFs, MIL-101(Cr) has a mesoporous molecular sieve structure and a large number of unsaturated Cr(III) sites, which could effectively bind with

electron-rich functional groups (Yang & Yan, 2011). In addition, MIL-101(Cr) is relatively stable under acidic and neutral conditions, which overcomes the shortcomings of water instability of some other MOFs such as MOF-5 and MOF-177, thus widening their applications in the pretreatment of traditional Chinese medicine (Jia et al., 2020). Although novel materials have been extensively investigated for environmental samples, limited studies have been conducted to remove heavy metals in medicinal herbs (Guo et al., 2020; Yanhong et al., 2017; Yufang & Danying, 2005; Xuejie Zhang et al., 2020). One of the main reasons might be the complex existing forms of heavy metals in medicinal herbs, such as complexation or embedding with matrix components. Besides, other problems can easily occur in the removal process, including secondary pollution, low adsorption capacity/efficiency, the difficulty of large-scale production, strict application requirements, and influences on effective components of medicinal herbs. Therefore, more studies are still needed to investigate adsorbents that can achieve good removal efficiency of heavy metals from medicinal herbs and simultaneously maintain their active ingredients.

This study aims to synthesize a magnetic nanomaterial to remove heavy metals from the decoction of *Ligusticum chuanxiong* Hort (*L. chuanxiong* Hort). The value of *L. chuanxiong* Hort ranked seventh in the export of Chinese herbal medicines, accounting for 2.68 % of the total export (Delin et al., 2019). As one of the representative medicinal herbs, *L. chuanxiong* Hort plays an essential role in the pharmaceutical industry with its abundant chemical components and unique pharmacological effects. It can be used to treat cardiovascular, cerebrovascular, respiratory, urinary, immune system, and gynecological diseases. Although *L. chuanxiong* Hort has unique properties in disease treatment and health care, the worldwide popularity of *L. chuanxiong* Hort has been hindered by the contamination of heavy metals mainly from polluted water, air, and soil (Fuyou et al., 2003; InSil et al., 2017). More than 30 literatures indicated the particularly severe contamination of cadmium in *L. chuanxiong* Hort (Delin et al., 2019). Since nanostructured composites have shown a good application prospect in heavy metals removal from plant extracts (Yongdi et al., 2019), the combination of magnetic nanoparticles and MOFs has been considered to realize the efficient removal of heavy metals from the decoction of *L. chuanxiong* Hort. Magnetic composites based on MOFs can inherit the excellent properties of MOFs and the rapid separation and recovery of magnetic material, thus avoiding the problems of secondary pollution or difficult separation/recycling of the adsorbents. As one of the most prominent MOFs, MIL-101(Cr), a chromium terephthalate solid characterized by cubic structure (Hupp & Poepelmeier, 2005), has shown excellent stability in the air, water, and a variety of organic solvents (Burtch et al., 2014). Hence, this study aims to synthesize an adsorbent based on $\text{Fe}_3\text{O}_4@\text{MIL-101}(\text{Cr})$ and evaluate its performance for heavy metals (Pb, Cd, As, Ni, and Zn ions) removal.

Considering the physicochemical property of these components, functionalization of $\text{Fe}_3\text{O}_4@\text{MIL-101}(\text{Cr})$ by polyethylene glycol (PEG) was intended to block the adsorption between the adsorbents and the effective components of *L. chuanxiong* Hort. PEG is a nanomaterial that is widely used to construct biosafety nanocarriers and functionalize other materials (Xuejie Zhang et al., 2020), which can improve the hydrophilicity and the dispersibility of the materials. Therefore, the introduction of PEG in the adsorbents was expected to guarantee sufficient contact between heavy metals and trapping

media and play as a barrier to separating the main effective components of *L. chuanxiong* Hort from the magnetic nanomaterial (Ostolska & Wisniewska, 2017). To the best of our knowledge, the PEG functionalized Fe₃O₄@MIL-101(Cr) (Fe₃O₄@MIL-101(Cr)@PEG) was applied to remove heavy metals from medicinal herbs for the first time. Specifically, the physicochemical properties of Fe₃O₄@MIL-101(Cr)@PEG were investigated. After the optimization of adsorption conditions, the adsorption mechanism was investigated by adsorption isotherm, kinetic and thermodynamic of heavy metals on Fe₃O₄@MIL-101(Cr)@PEG. Finally, the feasibility and reliability of heavy metals removal from the decoction of *L. chuanxiong* Hort were further studied and evaluated.

2. Materials and methods

2.1. Chemicals and materials

Iron chloride hexahydrate (FeCl₃·6H₂O, 99.0 %), chromium (III) nitrate nonahydrate (Cr(NO₃)₃·9H₂O, 99.0 %), dopamine hydrochloride (C₈H₁₁NO₂·HCl, 98.0 %), tris(hydroxymethyl) aminomethane (C₄H₁₁NO₃, ≥99.8 %), sodium hydroxide (NaOH, 97.0 %), terephthalic acid (C₈H₆O₄, 99.0 %), and phosphoric acid (H₃PO₄, ≥99.0 %) were purchased from Aladdin Biochemical Technology Co., Ltd. (Shanghai, China). Sodium acetate (C₂H₃NaO₂, 99.0 %), ethylene glycol (C₂H₆O₂, 98.0 %), and N, N-dimethylformamide (DMF, 99.5 %) were from Macklin Biochemical Co., Ltd. (Shanghai, China). Polyethylene glycol (PEG, 600 g/mol) was purchased from J&K Scientific Technology Co., Ltd. (Beijing, China). Hydrochloric acid (HCl, 36.0 ~ 38.0 %) and ethanol (C₂H₅OH, 99.7 %) were supplied by Chron Chemicals Co., Ltd. (Chengdu, China). Nitric acid (HNO₃, 70 %) was purchased from Crystal Clear Chemical Co., Ltd. (Suzhou, China). Acetonitrile (ACN, HPLC grade) was purchased from Sigma-Aldrich (Shanghai, China). Distilled water was purified by a Milli-Q system (Millipore Co.).

Arsenic standard stock solution (As⁵⁺, 1000 µg/mL, 2 % HNO₃), nickel standard stock solution (Ni²⁺, 1000 µg/mL, 5 % HNO₃), zinc standard stock solution (Zn²⁺, 1000 µg/mL, H₂O), cadmium standard stock solution (Cd²⁺, 1000 µg/mL, 5 % HNO₃), lead standard stock solution (Pb²⁺, 1000 µg/mL, 5 % HNO₃) were purchased from Henan R&D Center for certified reference material. Senkyunolide I (C₁₂H₁₆O₄, Sichuan Naturewill biotechnology Co., Ltd, 2203185901), Senkyunolide A (C₁₂H₁₆O₂, Chengdu Purifa technology development Co., Ltd, PRF8031301), and Ferulic acid (C₁₀H₁₀O₄, China Institute for identification of pharmaceutical and biological products, 110773-200611) were applied with the purity above 99.0 %. *L. chuanxiong* Hort samples were purchased from local pharmacies in Chengdu, China.

2.2. Instrument conditions

The analysis of heavy metals was performed by an inductively coupled plasma-optical emission spectrometer (ICP-OES, Agilent 5110). The following wavelengths of the measured elements were used: 188.980 nm (As), 231.604 nm (Ni), 213.857 nm (Zn), 214.439 nm (Cd), 220.353 nm (Pb). Other parameters of the ICP-OES were set as follows: forward power, 1.2 kW; plasma argon flow rate, 12.00 L/min; auxiliary

argon flow rate, 1.0 L/min; nebulizer argon flow rate, 0.7 L/min; read time, 10 s; stabilization time; 15 s.

The determination of active ingredients in the decoction of *L. chuanxiong* Hort was performed on a high-performance liquid chromatography system (HPLC, Thermo UltiMate 3000) connected with an ultraviolet detector. The chromatographic separation was realized by a Thermo BDS C18 column (4.6 mm × 250 mm, 5 µm). The mobile phase consisted of (A) acetonitrile and (B) water (containing 0.5 % phosphoric acid). Analyses were carried out with a gradient elution as follows: 10 %-16 % A at 0–15 min, 16 %-30 % A at 15–30 min, 30 %-40 % A at 30–35 min, 40 %-55 % A at 35–70 min. The detection wavelength was 276 nm. The injection volume was 10 µL. The column temperature and flow rate were set as 30 °C and 1.0 mL/min, respectively.

The in-house fabricated adsorbent was characterized by scanning electron microscopy (SEM, Hitachi SU8020), transmission electron microscopy (TEM, FEI Tecnai G2 F30), Fourier transform infrared spectroscopy (FT-IR, Nicolet IS10), X-ray diffraction (XRD, BRUCKER D8 ADVANCE) patterns, Vibrating Sample Magnetometer (VSM, BKT-4500), and specific surface area and porosity analyzer (Micromeritics ASAP 2460).

2.3. Synthesis of Fe₃O₄@MIL-101(Cr)@PEG

Polydopamine (PDA) has attracted much attention as a functional monomer owing to its unique coating ability and versatility (Duan et al., 2018). It can be self-polymerized onto magnetic nanoparticles under mild conditions to prepare adherent PDA films (Zhang et al., 2012; Zhao et al., 2015). The film with uniform thickness can be formed on various materials through the strong interaction with catechol and amine groups of dopamine (Bai et al., 2017). Therefore, PDA-coated magnetic nanoparticles were prepared as the substrate of MOFs in this study. The synthesis of Fe₃O₄@MIL-101(Cr)@PEG was referenced to our last work with some modification (Tang et al., 2022). Specifically, the synthetic route of magnetic MOF composites was as follows (Fig. 1): firstly, Fe₃O₄ magnetic microspheres were prepared by the solvothermal method according to the reference (Shao et al., 2012). Then, Fe₃O₄ microspheres were coated by a PDA layer via the polymerization of dopamine in the Tris-HCl buffer solution (pH = 8.5). The prepared Fe₃O₄@PDA was dissolved in deionized water containing a certain amount of Cr(NO₃)₃·9H₂O, terephthalic acid, and sodium acetate. The mixture was subsequently sealed in a Teflon-lined bomb and heated under 210 °C for 10 h. In this one-pot synthesis process, Cr(NO₃)₃·9H₂O provided metal nodes while terephthalic acid served as organic building blocks. The obtained Fe₃O₄@MIL-101(Cr) were successively washed with DMF, soaked in hot ethanol for 5 h, washed several times with ethanol, and dried under vacuum at 150 °C. After that, these dehydrated nanoparticles were suspended in PEG solution (1.5 mg/mL in water) and stirred at 30 °C for 4 h. The functionalized nanoparticles were recovered by applying an external magnet and washed twice with water to remove un-grafted PEG. Finally, the adsorbents were washed with ethanol and dried under vacuum at 30 °C.

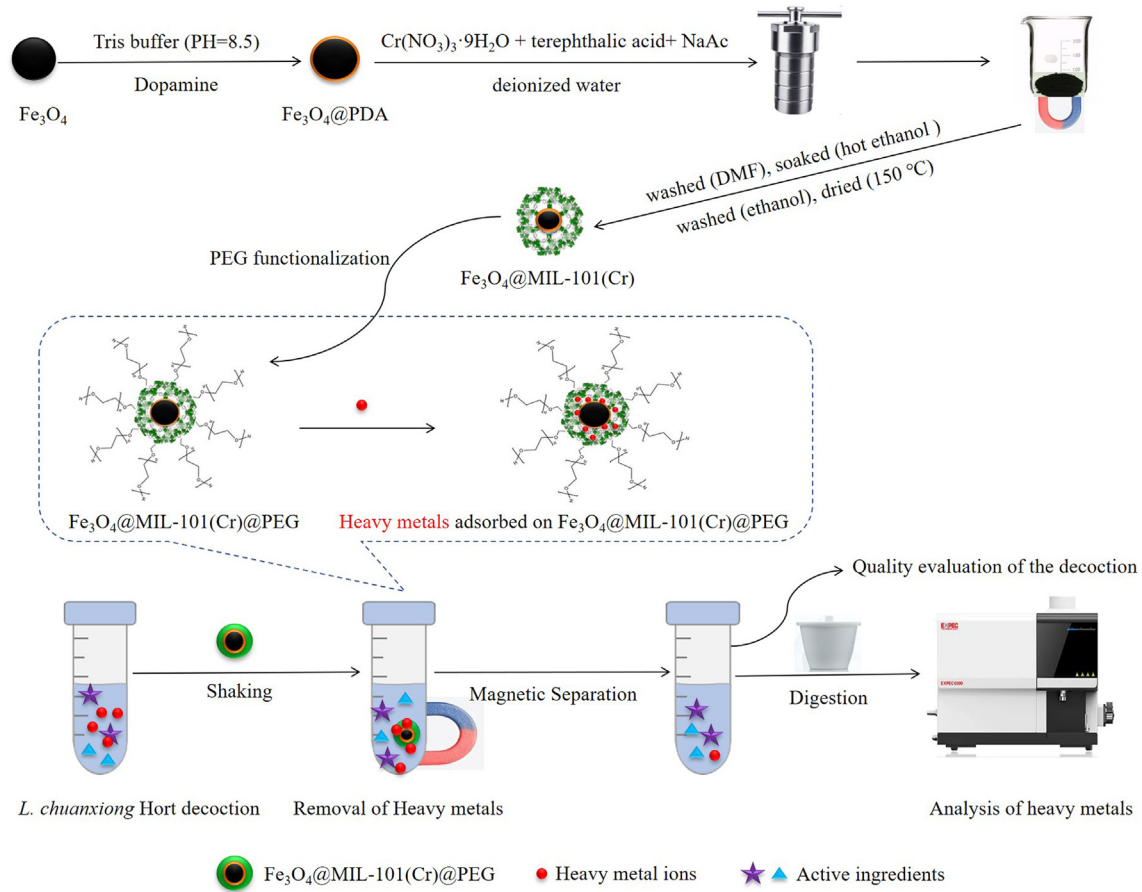


Fig. 1 Schematic of the preparation of Fe₃O₄@MIL-101(Cr)@PEG and its application for heavy metals removal.

2.4. Preparation of the decoction of *L. chuanxiong* Hort

L. chuanxiong Hort samples were randomly collected from local pharmacies. All samples were stored in sealed plastic bags below 4 °C for further use. The decoction of *L. chuanxiong* Hort was prepared as follows: 2.0 g of *L. chuanxiong* Hort was weighed accurately into a 250 mL polytetrafluoroethylene crucible. Then, 100 mL of ultrapure water was added to the crucible, boiled for 1 h, and separated from the samples. The last procedure was repeated twice. Finally, the combined decoction was filtered and concentrated under reduced pressure to 0.02 g/mL.

2.5. Adsorption behavior study

Adsorption kinetics, isotherms, and thermodynamic experiments were performed to evaluate the adsorption behavior of Fe₃O₄@MIL-101(Cr)@PEG toward As⁵⁺, Ni²⁺, Zn²⁺, Pb²⁺, and Cd²⁺ (Hayati et al., 2012; Xiong, Xue, et al., 2023). Specifically, the adsorption kinetics were carried out with 40 mg adsorbents in 50 mL of metal ion solutions (50 µg/mL of Pb, Cd, As, Ni, and Zn ions, pH = 5.36). After being shaken for a specific time interval (30–360 min), the kinetic factors were computed. The experimental adsorption data were modeled with the pseudo-first-order and pseudo-second-order kinetic models (Eq. (1) and (2), respectively):

$$\log(Q_e - Q_t) = \log Q_e - \frac{K_1}{2.303} t \quad (1)$$

$$\frac{t}{Q_t} = \frac{t}{Q_e} + \frac{1}{K_2 Q_e^2} \quad (2)$$

where Q_e (mg/g) and Q_t (mg/g) are the amounts of the adsorbed heavy metals on Fe₃O₄@MIL-101(Cr)@PEG at equilibrium and different times (min), respectively; K_1 (h⁻¹) and K_2 (g·mg⁻¹·min⁻¹) are the adsorption rate constants for the pseudo-first-order adsorption and pseudo-second-order adsorption, respectively.

The adsorption isotherms were carried out by adding 40 mg adsorbents into 50 mL of metal ions solution with various concentrations (0.8–100 µg/mL, PH = 5.36). Two well-known Langmuir and Freundlich isotherm models were applied to analyze the isotherm data (Eq. (3) and Eq. (4), respectively):

$$\frac{C_e}{Q_e} = \frac{C_e}{Q_m} + \frac{1}{K_L Q_m} \quad (3)$$

$$\log Q_e = \frac{1}{n_F} \log C_e + \log K_F \quad (4)$$

where Q_e is the quantity of the adsorbed heavy metals per gram of Fe₃O₄@MIL-101(Cr)@PEG at equilibrium (mg/g); Q_m is the maximum specific amount of heavy metals per gram of Fe₃O₄@MIL-101(Cr)@PEG (mg/g); C_e is the residual heavy met-

als concentration at equilibrium (mg/L); K_L is the Langmuir equilibrium constant (L/mg); K_F and n are indicators of adsorption capacity and adsorption intensity, respectively.

The thermodynamic adsorption parameters were also measured at different temperature (20 °C, 30 °C, and 40 °C). The mathematical relationship between ΔG , ΔH and ΔS were shown in Eq. (5). The thermodynamic linear relationship was shown in Eq. (6). The values of ΔH and ΔS can be calculated according to the intercept and slope of the fitting curve.

$$\Delta G = \Delta H - T\Delta S \quad (5)$$

$$\ln K = \frac{\Delta S}{R} - \frac{\Delta H}{RT} \quad (6)$$

where ΔG (kJ · mol⁻¹), ΔH (kJ · mol⁻¹), and ΔS (J · mol⁻¹ · K⁻¹) represent Gibbs free energy, enthalpy change, and entropy change of heavy metal ions adsorbed by the adsorbent, respectively; K is the thermodynamic equilibrium constant; T (K) is the temperature in Kelvin.

2.6. Removal and analysis of heavy metals in the decoction of *L. chuanxiong* Hort

As shown in Fig. 1, 40 mg of adsorbents were added to 50 mL of *L. chuanxiong* Hort decoction. The introduction of magnetism in the material allowed us to separate the adsorbent from the decoction of *L. chuanxiong* Hort by an external magnetic field. Therefore, the adsorbents were withdrawn by an external magnetic field after being shaken for a specific time interval. Then, the decoction was entirely transferred into a polytetrafluoroethylene crucible and digested with 0.5 mL nitric acid for 2 h. After digestion, the solution was further heated and concentrated to about 1 mL. Finally, the obtained concentrate was entirely transferred to a 10 mL volumetric flask and diluted with 2 % nitric acid solution to volume, which was ready for ICP-OES analysis. To compare the adsorption effect of heavy metal ions, the same experiments were conducted with Fe₃O₄ and MIL-101(Cr), respectively.

2.7. Reusability study

The regeneration and reusability of an adsorbent are imperative for its economic and practical applications. Thus, the adsorption–desorption cycles were repeated for some times to examine the regeneration efficiency of Fe₃O₄@MIL-101(Cr)@PEG. With the method described in section 2.6, the adsorption process was performed by adding 40 mg of adsorbents into 50 mL of spiked decoction with a concentration of 50 µg/mL and an adjusted pH value. After adsorption, the desorption of Pb, Cd, As, Ni, and Zn ions from the adsorbents was carried out with the aqueous HCl solution (0.1 M) as eluent. The Fe₃O₄@MIL-101(Cr)@PEG nanoparticles were stirred in the above solution for 1 h at room temperature. Then, the adsorbents were washed with distilled water several times for the next adsorption–desorption cycle. At the same time, the material after the first desorption was dried at 60 °C and weighed to obtain the recovery rate of the adsorbent.

2.8. Stability study

The stability of Fe₃O₄@MIL-101(Cr)@PEG nanoparticles against acidic solutions is vital for long-time practical

applications. Therefore, in the present work, the structural stability of this adsorbent against HCl (pH = 1) was studied for 10 h. Briefly, 100 mg Fe₃O₄@MIL-101(Cr)@PEG nanoparticles were added into 50 mL acidic, and the mixture was stirred at room temperature for 10 h (Ahmadijokani et al., 2021). After that, the nanoparticles were collected, washed with chloroform, and dried at 60 °C. Finally, the XRD diffractograms of the pristine adsorbents, the adsorbents after heavy metal adsorption, and the acid-treated adsorbents were compared to evaluate their structural stability.

2.9. Metal leaching rate

The adsorption process was performed by adding 40 mg of adsorbents into 50 mL of aqueous solution. It should be noted that no heavy metal standard solution was added in this process. After the same operation described in section 2.6, Fe and Cr ions were analyzed by ICP-OES.

2.10. Quality evaluation of the decoction of *L. chuanxiong* Hort

The content of the representative active ingredients, the solid content, and the HPLC fingerprints similarity were used as the quality monitoring indicators of *L. chuanxiong* decoction before and after the removal of heavy metals.

2.10.1. Determination of Senkyunolide I, Senkyunolide A, and Ferulic acid

Senkyunolide I, Senkyunolide A, and Ferulic acid were chosen as representative active ingredients of the decoction of *L. chuanxiong* Hort. These compounds were analyzed and compared in the decoction before and after removing heavy metals based on HPLC analysis. The HPLC parameters were described in section 2.2.

2.10.2. Analysis of the solid content

25 mL of *L. chuanxiong* Hort decoction before and after treatment were respectively transferred to an evaporation dish that was dried to constant weight and evaporated to dryness in a boiling water bath. Then, the solid content was weighed and measured.

2.10.3. Evaluation of HPLC fingerprints similarity

The *L. chuanxiong* Hort decoction was analyzed by HPLC before and after the removal of heavy metals. Then, the similarity of HPLC fingerprints was evaluated by the similarity evaluation system for the chromatographic fingerprints of traditional Chinese medicine (2012 Edition).

3. Results and discussion

3.1. Characterization of Fe₃O₄@MIL-101(Cr)@PEG

The FT-IR spectrum of the in-house fabricated material is shown in Fig. S1. It exhibited the FT-IR spectra of Fe₃O₄, Fe₃O₄@PDA, Fe₃O₄@MIL-101(Cr), Fe₃O₄@MIL-101(Cr)@PEG, and MIL-101(Cr). In the spectrum of Fe₃O₄, the characteristic absorption peak at 606 cm⁻¹ was attributed to the Fe-O-Fe vibration. The two broad bands at 3457 cm⁻¹ and 1640 cm⁻¹ were respectively assigned to O—H stretching and

bending vibrations of water, which were probably located on the surface of iron oxide nanoparticles (Shahabadi et al., 2016). In addition to the typical peaks of Fe_3O_4 , many new peaks can be seen in the spectrum of $\text{Fe}_3\text{O}_4@\text{PDA}$. Representatively, the peak at 630 cm^{-1} was ascribed to the N—H bending vibration. The unique absorption bands near 1290 and 1500 cm^{-1} were related to the bending vibration of C—N and the stretching vibration of the aromatic ring, respectively. These features showed that the PDA had been successfully coated on the surface of Fe_3O_4 . As for MIL-101(Cr), the band at 1021 cm^{-1} was corresponded to the in-plane bend vibrations of terephthalic acid. The deformation vibration belonging to C—H at 1150 , 1013 , 889 , 751 cm^{-1} was consistent with the reported peaks of MIL-101(Cr) in literature (Qiu et al., 2020). And as for $\text{Fe}_3\text{O}_4@\text{MIL-101(Cr)}$, the characteristic vibration bands of O—C—O (around 1385 and 1624 cm^{-1}) indicated the existence of the terephthalic acid within MIL-101(Cr) and the connection of the carboxylate ligand to the Cr metal center, which could be obtained in MIL-101(Cr) spectrum (Yalcin & Kayan, 2012). The broad band near 585 cm^{-1} confirmed the incorporation of the Fe-O-Fe group in the nanocomposite (Madhuri et al., 2005). As for $\text{Fe}_3\text{O}_4@\text{MIL-101(Cr)@PEG}$, the shifting and increased intensity of the peak in the region $3500\text{--}3300\text{ cm}^{-1}$ indicated the enhanced hydrogen bonding induced by the hydroxyl groups of PEG. The results demonstrated the successful fabrication of $\text{Fe}_3\text{O}_4@\text{MIL-101(Cr)@PEG}$.

The morphology of $\text{Fe}_3\text{O}_4@\text{MIL-101(Cr)}$ and $\text{Fe}_3\text{O}_4@\text{MIL-101(Cr)@PEG}$ was investigated by SEM and TEM. As described in our last work, the MIL-101(Cr) was verified to be randomly extended around $\text{Fe}_3\text{O}_4@\text{PDA}$ (Fig. S2a and Fig. S2c) (Tang et al., 2022). In comparison to $\text{Fe}_3\text{O}_4@\text{MIL-101(Cr)}$, a rougher surface was obviously observed for $\text{Fe}_3\text{O}_4@\text{MIL-101(Cr)@PEG}$, which was speculated to be the extension of PEG around the $\text{Fe}_3\text{O}_4@\text{MIL-101(Cr)}$ (Fig. S2b). The TEM image of $\text{Fe}_3\text{O}_4@\text{MIL-101(Cr)@PEG}$ further verified that PEG was loaded around $\text{Fe}_3\text{O}_4@\text{MIL-101(Cr)}$ to construct a core-shell structure (Fig. S2d). The results showed that a larger specific surface area was obtained after the modification of $\text{Fe}_3\text{O}_4@\text{MIL-101(Cr)}$ by PEG. Besides, the overlapped and agglomerated PEG provided a restricted-access structure, which was beneficial for specifically trapping heavy metals.

Since the specific surface area is another important property of adsorbent material, the porous structure and property of $\text{Fe}_3\text{O}_4@\text{MIL-101(Cr)@PEG}$ were tested in this study. Generally, type IV isotherm is generated by mesoporous solids. A typical feature is that the adsorption branch of the isotherm is inconsistent with the desorption branch of the isotherm, and a hysteresis loop can be observed. In this study, a type IV curve with a small hysteresis was provided as the N_2 adsorption-desorption isotherm of the material in Fig. S3, indicating the typical property of a mesoporous structure. The Brunauer-Emmett-Teller (BET) surface area was $248.5447\text{ m}^2/\text{g}$, which was satisfactory for enrichment purposes. Moreover, the total pore volume was calculated to be $0.17\text{ cm}^3/\text{g}$ by the Barrett-Joyner-Halenda method. The average pore diameter of the amorphous nanomaterial was about 4.59 nm . The results have verified that the in-house fabricated $\text{Fe}_3\text{O}_4@\text{MIL-101(Cr)@PEG}$ had a high surface area, large pore volume, and narrow pore diameter. According to the above results, the $\text{Fe}_3\text{O}_4@\text{MIL-101(Cr)@PEG}$ was characterized by beneficial structure

and properties for adsorption and separation of heavy metals, which was simultaneously expected to avoid the influence on the active ingredients.

XRD patterns were used to identify the crystal structure of the synthesized nanomaterials (Xiong, Liu, et al., 2023). Fig. S4 exhibited the XRD patterns of MIL-101(Cr) and $\text{Fe}_3\text{O}_4@\text{MIL-101(Cr)@PEG}$. The sharp diffraction peaks indicated that the MIL-101(Cr) was a material with high crystallinity. The obvious peaks at 2θ of 5.0° , 5.9° , 9.8° , 10.5° , represented the reflections of typical MIL-101(Cr) (Li et al., 2020). After intercalating Fe_3O_4 nanoparticles into MIL-101(Cr), the characteristic peaks of Fe_3O_4 at 30.0° , 35.4° , 54.5° , 63.2° , 67.6° could be observed (Davodi et al., 2019). Obviously, the characteristic diffraction peaks of MIL-101(Cr) were presented in the $\text{Fe}_3\text{O}_4@\text{MIL-101(Cr)@PEG}$, indicating that the Fe_3O_4 nanoparticles didn't change the high crystallinity of MIL-101(Cr) (Abutalib & A. Rajeh, 2020). In addition, the peak at 2θ of 19.1° was the characteristic peak of PEG (Zheng et al., 2021), which coincided with the peak of MIL-101(Cr). But it could be confirmed from the intensity of the peak that it was the characteristic peak of PEG. All these characterizations supported the successful preparation of the $\text{Fe}_3\text{O}_4@\text{MIL-101(Cr)@PEG}$ nanocomposites.

The magnetic properties of the Fe_3O_4 and $\text{Fe}_3\text{O}_4@\text{MIL-101(Cr)@PEG}$ were studied using a VSM in an external magnetic field from $-12,000\text{ Gs}$ to $+12,000\text{ Gs}$. As shown in Fig. S5, the hysteresis loops of Fe_3O_4 and $\text{Fe}_3\text{O}_4@\text{MIL-101(Cr)@PEG}$ were no hysteresis, which showed no remanence or coercivity at room temperature. The results exhibited the typical superparamagnetic character of both materials. The maximal saturation magnetization of Fe_3O_4 was 62.98 emu/g . As for $\text{Fe}_3\text{O}_4@\text{MIL-101(Cr)@PEG}$, the saturation magnetization decreased to 40.42 emu/g . Although the saturation magnetization was lower than that of bulk magnetite (92 emu/g) (Han et al., 1994), the particles were only redispersed under slight shaking when the magnetic field was removed. This feature facilitated collection, regeneration, and reutilization of the materials. Thus, it could ensure the easy separation of $\text{Fe}_3\text{O}_4@\text{MIL-101(Cr)@PEG}$ from the aqueous solution with a low magnetic field. These structural characteristics and magnetic behavior make $\text{Fe}_3\text{O}_4@\text{MIL-101(Cr)@PEG}$ nanocomposites great potential as a good adsorbent for removing heavy metals from Chinese medicinal materials.

3.2. Removal of heavy metals in the decoction of *L. chuanxiong* Hort

Parameters that can influence the removal efficiency of the heavy metal ions were initially investigated. All experiments were conducted in triplicate with 50 mL of spiked *L. chuanxiong* Hort decoction, of which the pH was adjusted with NaOH solution. The spiked concentration of each heavy metal ion was $50\text{ }\mu\text{g/mL}$, including Pb, Cd, As, Ni, and Zn ions. At the same time, parallel experiments were conducted on *L. chuanxiong* Hort decoction without spiking heavy metals for the deduction of background.

3.2.1. Effect of pH

The solution pH is a key factor for the adsorption removal of heavy metal ions since it could affect the existing forms of heavy metals and the surface charge of the adsorbents by

changing the protonation degree of its functional groups. Therefore, the influence of solution pH on the removal efficiency of Fe₃O₄@MIL-101(Cr)@PEG toward Pb²⁺, Cd²⁺, As⁵⁺, Zn²⁺, and Ni²⁺ is worth studying. In optimization of pH (pH 2–pH 8), the adsorption time and the adsorbent amount were 60 min and 25 mg, respectively. As shown in Fig. 2A, Fe₃O₄@MIL-101(Cr)@PEG exhibited better adsorption performance toward Pb²⁺, Cd²⁺, and As⁵⁺ in a suitable pH range. It displayed that the removal efficiency of Fe₃O₄@MIL-101(Cr)@PEG for all heavy metal ions was lower at low pH and enhanced with increasing pH within a certain range. At the highly acidic solutions, the amine groups and oxygen atoms with lone electrons in the material would be protonated due to the existence of many hydrogen ions. Thus, the positively charged groups on the surface of the adsorbents may repulse the positively charged metal ions. Moreover, H₃O⁺ ions competed with other adsorbate ions for the vacant binding sites on the adsorbents in acidic media. As a consequence, the removal efficiency of all metal ions decreased in conditions of low pH (Kayan & Kayan, 2022). Although the surface

charge of the adsorbents may be negative at higher pH, the interactions seemed to be reduced between heavy metal ions and the adsorbents, which might be ascribed to the charge neutralization between the heavy metal and hydroxyl ions. In summary, the removal efficiency increased from pH 2 to pH 6 while slightly decreased from pH 6 to pH 8. It is worth mentioning that the actual pH value of *L. chuanxiong* Hort decoction is 5.36. The removal efficiency of the heavy metal ions was additionally tested at pH 5.36. As can be seen from the result, the best removal efficiency was obtained at pH 5.36 for Pb²⁺, while pH 6 for As⁵⁺ and Ni²⁺. Besides, the removal efficiency was almost the same for Zn²⁺ and Cd²⁺ at two pH values. Comprehensively considering the removal efficiency and the convenience of practical application, the original pH of the decoction (pH 5.36) was applied in the following experiment.

3.2.2. Effect of adsorption time

The adsorption time was evaluated in the range of 30–360 min. In optimization of adsorption time, the solution pH and the adsorbent amount were applied as 5.36 and 25 mg, respec-

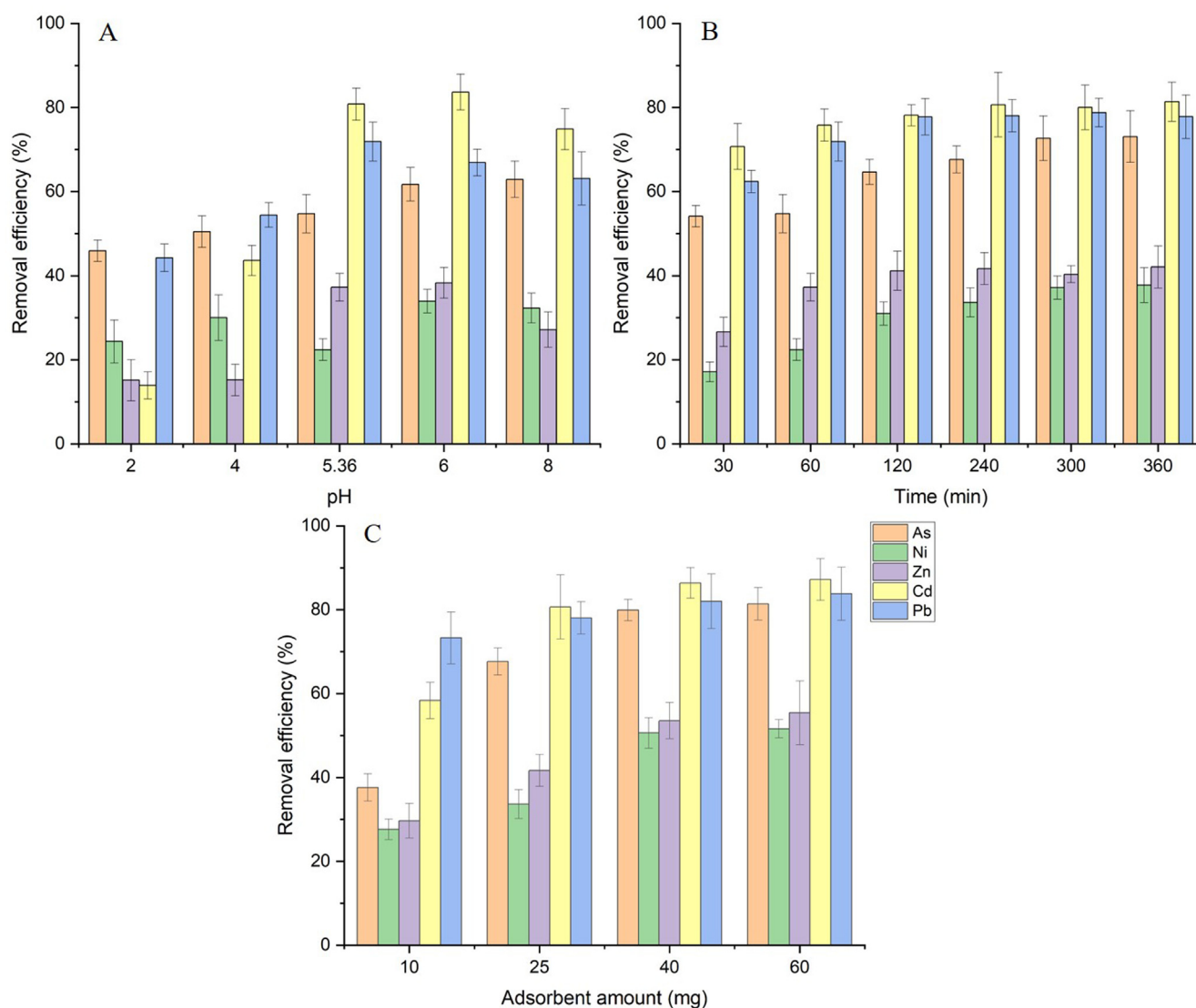


Fig. 2 Effect of (A) solution pH, (B) adsorption time, and (C) adsorbent amount on the removal efficiency of heavy metals.

tively. Fig. 2B displayed the effect of the adsorption time on the removal efficiency of As, Ni, Zn, Cd, and Pb ions. It can be found that the removal rate was proportional to the adsorption time in a certain adsorption time. The removal efficiency

of Zn^{2+} , Cd^{2+} , and Pb^{2+} almost remained the same from the adsorption time of 240 min, and the removal efficiency of Ni^{2+} and As^{5+} reached the equilibrium at the adsorption time of 300 min. Specifically, the adsorption rates followed

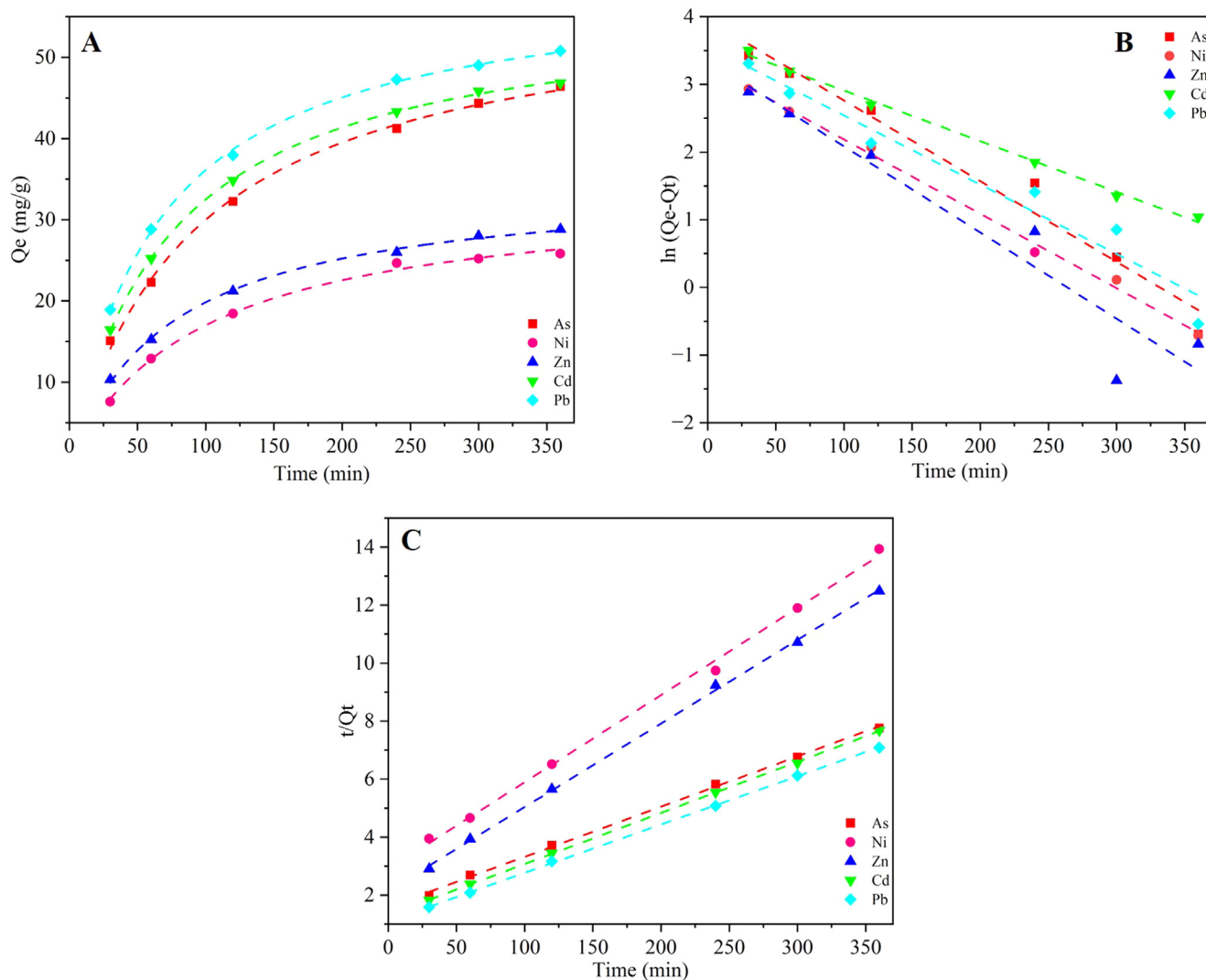


Fig. 3 The adsorption kinetics of As^{5+} , Ni^{2+} , Zn^{2+} , Cd^{2+} , and Pb^{2+} onto $\text{Fe}_3\text{O}_4@\text{MIL-101}(\text{Cr})@\text{PEG}$ (A) and fitted lines with pseudo-first-order (B) and pseudo-second-order (C).

Table 1 Kinetic factors of $\text{Fe}_3\text{O}_4@\text{MIL-101}(\text{Cr})@\text{PEG}$ toward five heavy metal ions.

Kinetic models	Metal ions	R^2	Q_e (mg/g)	K
Pseudo-first-order	As	0.9835	45.90 ± 1.33	0.0109 ± 0.0010
	Ni	0.9965	26.33 ± 0.37	0.0108 ± 0.0005
	Zn	0.9802	28.27 ± 0.75	0.0128 ± 0.0012
	Pb	0.9808	49.67 ± 1.20	0.0139 ± 0.0012
	Cd	0.9883	46.37 ± 0.96	0.0128 ± 0.0009
Pseudo-second-order	As	0.9974	57.83 ± 1.07	0.0002 ± 0.00001
	Ni	0.9954	33.45 ± 0.87	0.0003 ± 0.00003
	Zn	0.9978	34.61 ± 0.49	0.0004 ± 0.00002
	Pb	0.9989	59.91 ± 0.55	0.0003 ± 0.00001
	Cd	0.9948	56.83 ± 0.33	0.0002 ± 0.00005

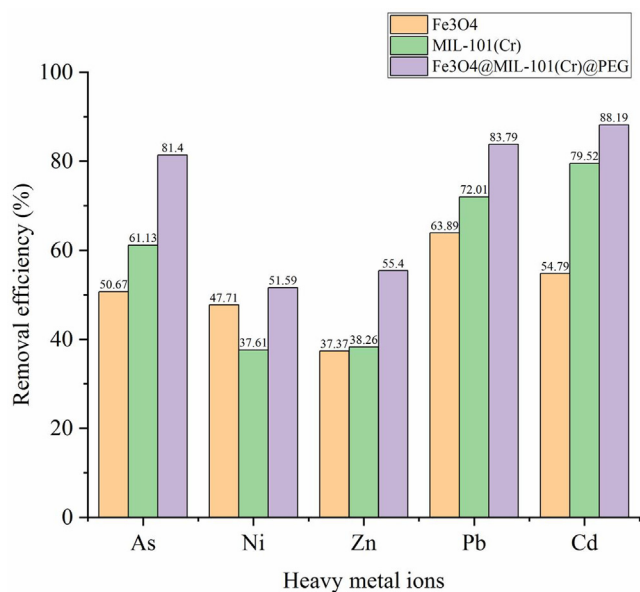


Fig. 4 The removal efficiency of Fe₃O₄, MIL-101(Cr), and Fe₃O₄@MIL-101(Cr)@PEG for five heavy metal ions.

the sequence: $\text{Cd}^{2+} \approx \text{Pb}^{2+} > \text{As}^{5+} > \text{Zn}^{2+} > \text{Ni}^{2+}$, which could be due to the difference in the hydrated radius, electronegativity, and acid-base properties. To sum up, the best adsorption time was 240 min.

Furthermore, based on Fig. 3 and the data summarized in Table 1, it was evident that the pseudo-second-order kinetic model was more suitable for describing the heavy metals adsorption on Fe₃O₄@MIL-101(Cr)@PEG, suggesting that the adsorption of heavy metals on the Fe₃O₄@MIL-101(Cr)@PEG mainly occurred through chemical adsorption (Xue Zhang et al., 2020). The chemical adsorption probably involved the electrons exchange and sharing ($-\text{OH}$, $-\text{NH}_3$, strong chelating groups), and covalent interactions of active sites with metal ions (As^{5+} , Ni^{2+} , Zn^{2+} , Cd^{2+} , and Pb^{2+}) (Xiong et al., 2020; Xiong et al., 2021; Xue Zhang et al., 2020).

3.2.3. Effect of adsorbent amount

The adsorbent amount is another crucial parameter affecting the removal efficiency of heavy metals. The effect of the adsorbent amount was investigated in the range from 10 mg to 60 mg. In optimization of adsorbent amount, the solution pH and the adsorption time were 5.36 and 240 min, respectively. Generally, the ratio of adsorbate ions to adsorbent

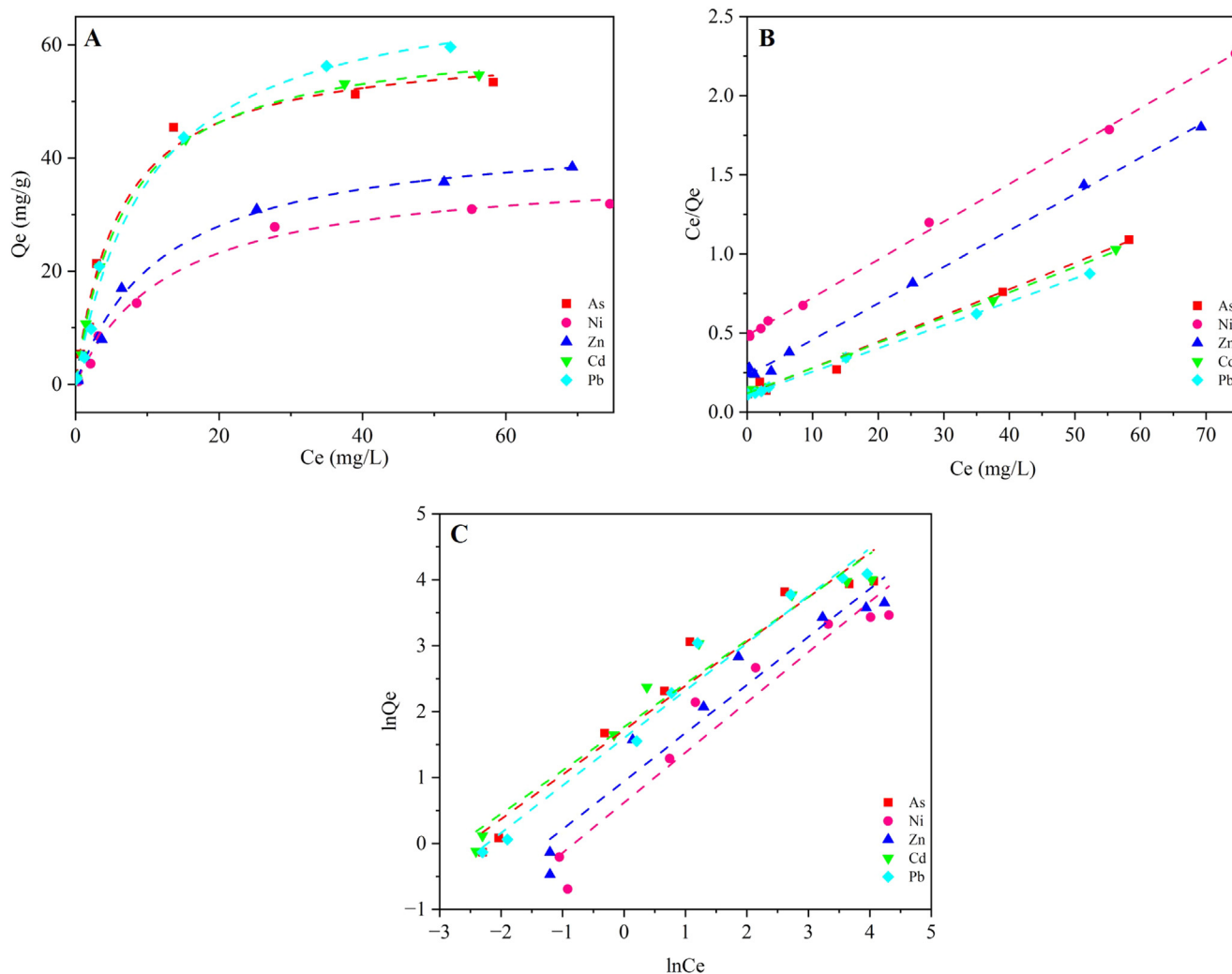


Fig. 5 (A) The adsorption isotherms of As^{5+} , Ni^{2+} , Zn^{2+} , Cd^{2+} , and Pb^{2+} onto Fe₃O₄@MIL-101(Cr)@PEG, (B) fitted lines with the Langmuir model, and (C) fitted lines with the Freundlich model.

Table 2 Isotherm parameters for the adsorption removal of five heavy metal ions on Fe₃O₄@MIL-101(Cr)@PEG.

Isotherm models	Constants	Heavy metal ions				
		As	Ni	Zn	Pb	Cd
Langmuir	Q _m (mg/g)	60.27 ± 2.68	38.48 ± 1.58	45.06 ± 1.71	72.18 ± 3.28	62.29 ± 0.91
	K _L (L/mg)	0.1656 ± 0.0277	0.0758 ± 0.0103	0.0818 ± 0.0103	0.0979 ± 0.0142	0.1442 ± 0.0079
	R ²	0.9872	0.9924	0.9935	0.9923	0.9988
	R _L	0.057–0.883	0.1166–0.9428	0.1089–0.9386	0.0927–0.9274	0.0649–0.8966
Freundlich	K _F (mg/g)	11.8986 ± 3.0280	4.9135 ± 1.2962	5.9556 ± 1.3472	9.8464 ± 2.2955	11.2755 ± 2.3451
	1/n _F	0.3940 ± 0.0716	0.4559 ± 0.0686	0.4558 ± 0.0597	0.4763 ± 0.0664	0.4155 ± 0.0587
	R ²	0.9119	0.9413	0.9565	0.9494	0.9519

Table 3 Comparison of the maximum adsorption capacity of different adsorbents toward five heavy metal ions.

Adsorbent	Adsorption capacity (mg/g)					Reference
	As ⁵⁺	Ni ²⁺	Zn ²⁺	Pb ²⁺	Cd ²⁺	
UiO-66-NHC(S)NHMe	–	–	–	232	49	(Saleem et al., 2016)
HFB	–	12.13	22.25	2.89	22.03	(Shin, 2017)
Denim textile wastes	1.50	–	25.50	–	14.83	(Mendoza-Castillo et al., 2015)
Granular activated carbon	2.50	–	–	–	–	(Natale et al., 2008)
Fe ₃ O ₄ /Mg-Al-CO ₃ -LDH	–	–	–	–	54.7	(Shan et al., 2015)
Rice husk ash	–	–	14.30	–	–	(Ahmaruzzaman, 2011)
LDH-Cl	–	–	–	108	61	(González et al., 2015)
Modified waste silk	–	7.47	–	–	8.03	(Mia et al., 2022)
Chitosan	–	–	–	7.70	–	(Cheng & Lin, 2006)
Fe ²⁺ -loaded activated carbon	2.02	–	–	–	–	(Tuna et al., 2013)
Iron-modified carbon	1.25	–	–	–	–	(Vitela-Rodriguez & Rangel-Mendez, 2013)
Dashukivskij bentonite	–	–	–	52.08	26.04	(Kostenko et al., 2019)
Poultry litter	–	52	80	–	–	(Kucharski et al., 2021)
MgAL-LDH	–	–	–	12	18.25	(Xue Zhang et al., 2020)
Hybrid material-A	–	–	14.29	38.76	–	(Cerraholu et al., 2018)
Hybrid material-B	–	–	25.61	38.09	–	(Cerraholu et al., 2018)
Fe ₃ O ₄ @MIL-101(Cr)@PEG	60.27 ± 2.68	38.48 ± 1.58	45.06 ± 1.71	72.18 ± 3.28	62.29 ± 0.91	This work

vacancies was reduced by increasing the adsorbent dosage. Thus, the removal efficiency increased with the adsorbent amount, as shown in Fig. 2C. However, at higher adsorbent dosages, the available vacancies may be reduced due to the aggregation of the adsorbent nanoparticles. The removal efficiency was accordingly predicted to decrease. In this study, the removal efficiency of As⁵⁺, Ni²⁺, Zn²⁺, Cd²⁺, and Pb²⁺ were close to the maximum when the adsorbent amount was 40 mg. With the adsorbent amount continually increasing from 40 mg to 60 mg, the removal efficiency of heavy metals remained basically unchanged.

In summary, the optimized parameters were obtained as follows: pH 5.36, adsorption time of 240 min, and adsorbent amount of 40 mg. Under the optimal conditions and the spiked concentration of 50 µg/mL, the removal efficiency of Fe₃O₄@MIL-101(Cr)@PEG for As⁵⁺, Ni²⁺, Zn²⁺, Cd²⁺, and Pb²⁺ were 81.40 %, 51.59 %, 55.40 %, 88.19 %, and 83.79 %, respectively. It indicated that the in-house fabricated adsorbent had excellent removal efficiency for As⁵⁺, Cd²⁺, and Pb²⁺ in the decoction of *L. chuanxiong* Hort, while obvious removal efficiency for Ni²⁺ and Zn²⁺.

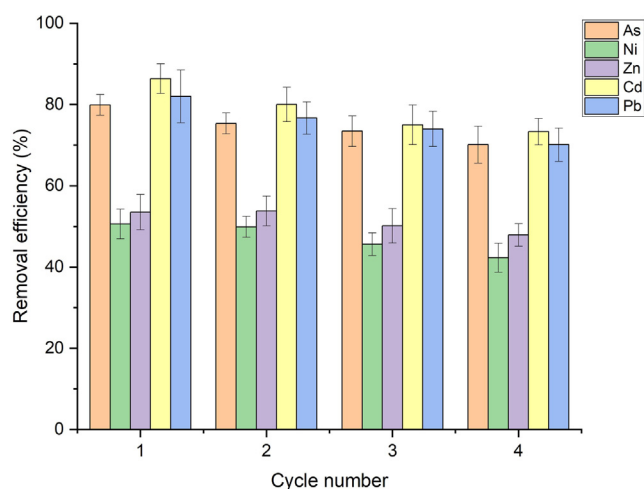
To further assess the removal efficiency of the Fe₃O₄@MIL-101(Cr)@PEG, comparison with Fe₃O₄ and MIL-101(Cr) was carried out under the same conditions. As can be seen in Fig. 4, the Fe₃O₄@MIL-101(Cr)@PEG exhibited the highest removal efficiency for As⁵⁺, Ni²⁺, Zn²⁺, Cd²⁺, and Pb²⁺.

3.2.4. Adsorption isotherms

Adsorption isotherms are critical for the overall improvement of adsorption mechanism pathways and the effective design of an adsorption system. The isotherm data are analyzed using the Langmuir and Freundlich models. The relevant results were depicted in Fig. 5, and the measured parameters were compiled in Table 2. As presented in Fig. 5A, the adsorption capacity of Fe₃O₄@MIL-101(Cr)@PEG toward As⁵⁺, Ni²⁺, Zn²⁺, Cd²⁺, and Pb²⁺ increased rapidly with an increase in their initial concentrations till the plots reach a plateau and remained relatively constant. The emergence of the plateau signifies that active sites were fully saturated (Ahmadijokani et al., 2021). Fig. 5 unfolded that the Langmuir isotherm model matched the experimental results.

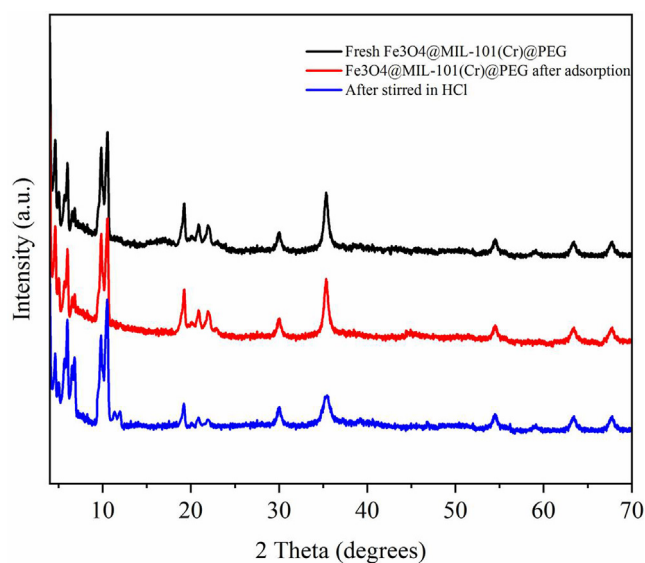
Table 4 Thermodynamic parameters for the adsorption removal of five heavy metal ions on Fe₃O₄@MIL-101(Cr)@PEG at different temperatures.

Temperature (°C)	Constants	Heavy metal ions				
		As	Ni	Zn	Pb	Cd
20	$\Delta G(\text{kJ}\cdot\text{mol}^{-1})$	-24.33	-7.11	-8.98	-17.22	-21.89
	$\Delta H(\text{kJ}\cdot\text{mol}^{-1})$	-17.65	-2.95	-3.84	-6.02	-14.12
	$\Delta S(\text{J}\cdot\text{mol}^{-1}\cdot\text{K}^{-1})$	-41.07	-1.18	-2.27	-4.27	-29.93
	Q_m (mg/g)	60.27 ± 2.68	38.48 ± 1.58	45.06 ± 1.71	72.18 ± 3.28	62.29 ± 0.91
	R^2	—	—	—	—	—
30	$\Delta G(\text{kJ}\cdot\text{mol}^{-1})$	-19.75	-7.04	-8.81	-16.43	-18.60
	$\Delta H(\text{kJ}\cdot\text{mol}^{-1})$	—	—	—	—	—
	$\Delta S(\text{J}\cdot\text{mol}^{-1}\cdot\text{K}^{-1})$	—	—	—	—	—
	Q_m (mg/g)	55.02 ± 1.34	27.77 ± 0.83	34.76 ± 1.80	62.92 ± 3.10	55.82 ± 2.88
	R^2	0.9998	0.9949	0.9995	0.9999	0.9992
40	$\Delta G(\text{kJ}\cdot\text{mol}^{-1})$	-16.36	-7.03	-8.68	-15.71	-16.15
	$\Delta H(\text{kJ}\cdot\text{mol}^{-1})$	—	—	—	—	—
	$\Delta S(\text{J}\cdot\text{mol}^{-1}\cdot\text{K}^{-1})$	—	—	—	—	—
	Q_m (mg/g)	47.18 ± 1.21	19.62 ± 0.71	26.92 ± 1.35	54.32 ± 2.92	50.19 ± 1.05
	R^2	—	—	—	—	—

**Fig. 6** Reusability of the in-house fabricated Fe₃O₄@MIL-101(Cr)@PEG.

Same conclusion was presented in Table 2. It implied that the adsorption of As⁵⁺, Ni²⁺, Zn²⁺, Cd²⁺, and Pb²⁺ onto the Fe₃O₄@MIL-101(Cr)@PEG was monolayer. There was no interaction between adsorbate ions, and the surface of the adsorbent was homogeneous (Yuan et al., 2017). As can be seen from Table 2, the calculated R_L and $1/n_F$ were between 0 and 1, indicating that the adsorption process was favorable and Fe₃O₄@MIL-101(Cr)@PEG was a good adsorbent for heavy metals removal from aqueous solution. This result suggested that the adsorption process of Fe₃O₄@MIL-101(Cr)@PEG toward As⁵⁺, Ni²⁺, Zn²⁺, Cd²⁺, and Pb²⁺ was monolayer coverage adsorption and favorable (Mahmoodi & Mohammad, 2015; Xue Zhang et al., 2020).

Moreover, the maximum adsorption capacity of the adsorbent toward the heavy metals was compared with the literature data in Table 3. The adsorption capacity of the five heavy metal ions on Fe₃O₄@MIL-101(Cr)@PEG was equal to or better than other adsorbents. Some data showed that the adsorption capacity of this material for heavy metal ions was

**Fig. 7** XRD patterns of Fe₃O₄@MIL-101(Cr)@PEG before and after being used in different conditions.

lower than that of other materials, and it was because those other materials only target one or two heavy metal ions, which greatly reduced the competition for material adsorption sites.

The temperature of an adsorption system is associated with adsorption thermodynamics and affects the adsorption efficiency. Thermodynamic adsorption parameters were measured and shown in Table 4. It can be seen that the theoretical maximum adsorption amount (Q_m) of five heavy metals on Fe₃O₄@MIL-101(Cr)@PEG decreased in turn with an increase in temperature from 20 °C to 40 °C, indicating that lowering the temperature was beneficial to the adsorption process. This phenomenon can be explained by the negative values of ΔH of As⁵⁺, Ni²⁺, Zn²⁺, Cd²⁺, and Pb²⁺, which implied that the adsorption process was exothermic. Hence, lowering the temperature was conducive to adsorption. As for the ΔG values all less than zero at different temperatures, it indicated that

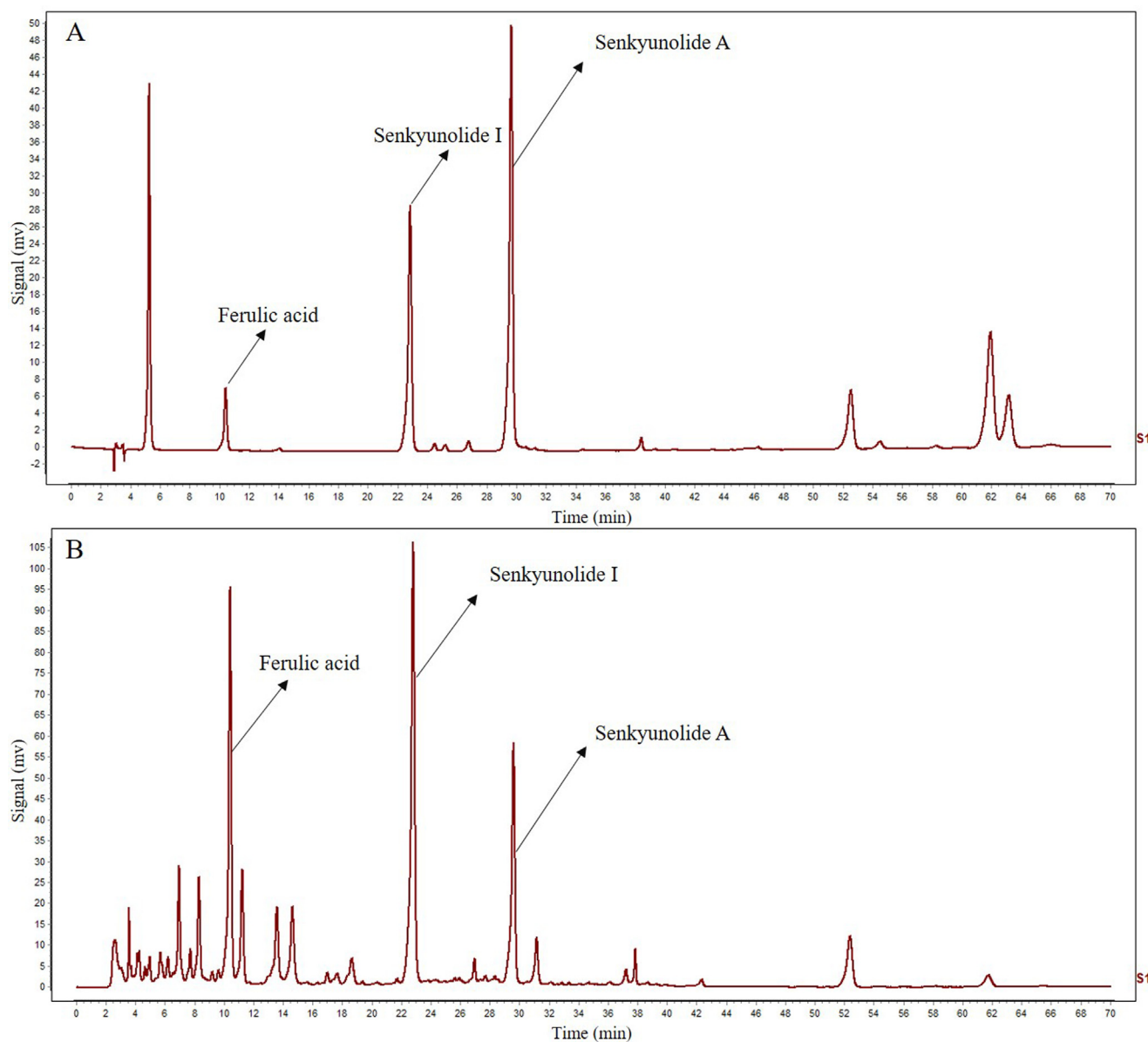


Fig. 8 HPLC chromatogram of (A) the mixed standard and (B) the testing sample.

the adsorption process was spontaneous. In addition, the negative values of ΔS indicated that the degree of freedom of the interface between $\text{Fe}_3\text{O}_4@\text{MIL-101}(\text{Cr})@\text{PEG}$ and the aqueous solution decreased during the adsorption process. To sum up, the adsorption of As^{5+} , Ni^{2+} , Zn^{2+} , Cd^{2+} , and Pb^{2+} by $\text{Fe}_3\text{O}_4@\text{MIL-101}(\text{Cr})@\text{PEG}$ was a spontaneous, exothermic, and entropy decreasing process.

3.3. Adsorbent reusability

The reusability of the adsorbent was investigated by adsorption–desorption cycle experiments, which was an important parameter to evaluate the applicability of $\text{Fe}_3\text{O}_4@\text{MIL-101}(\text{Cr})@\text{PEG}$. As shown in Fig. 6, the removal efficiency for As, Ni, Zn, Pb, and Cd ions almost remained unchanged after four consecutive adsorption–desorption cycles. The relative standard deviations (RSDs) were calculated to be 5.47 % (As^{5+}),

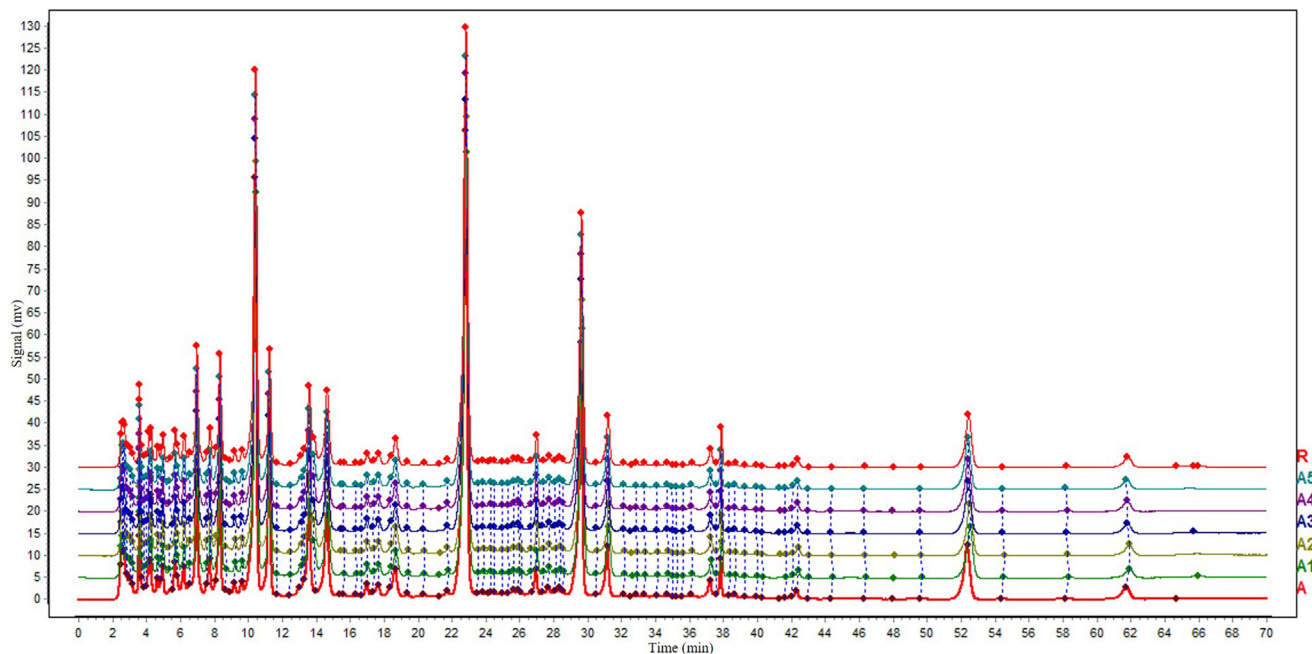
8.27 % (Ni^{2+}), 5.51 % (Zn^{2+}), 7.45 % (Cd^{2+}), and 6.60 % (Pb^{2+}), respectively. It was demonstrated that the removal efficiency of $\text{Fe}_3\text{O}_4@\text{MIL-101}(\text{Cr})@\text{PEG}$ for As, Ni, Zn, Pb, and Cd ions had been well restored at least for four cycles. The result indicated that the in-house fabricated $\text{Fe}_3\text{O}_4@\text{MIL-101}(\text{Cr})@\text{PEG}$ had good reusability and a great potential for sustainable heavy metals removal. In addition, the amount of material after the first heavy metal desorption was 34.4 mg. The loss rate was only 14 %, which meant that the recovery rate of the material was 86 %. In this way, only a small amount of adsorbents was added in successive experiment. In general, the recovery rate of the adsorbent was satisfactory.

3.4. Adsorbent stability

The XRD patterns of $\text{Fe}_3\text{O}_4@\text{MIL-101}(\text{Cr})@\text{PEG}$ were shown in Fig. 7. After being used in different solutions (HCl

Table 5 Content of the active ingredients in the decoction of *L. chuanxiong* Hort before and after the heavy metal removal.

Compounds	Quality score (%)					Rate of change (%)	
	Control	Sample 1	Sample 2	Sample 3	Sample 4		Sample 5
Ferulic acid	0.1300	0.1189	0.1216	0.1211	0.1211	0.1207	7.18
Senkyunolide I	0.0459	0.0443	0.0456	0.0448	0.0459	0.0447	1.93
Senkyunolide A	0.1283	0.1213	0.1245	0.1234	0.1240	0.1223	4.09

**Fig. 9** Similarity evaluation on HPLC fingerprints of *L. chuanxiong* decoction with (A₁₋₅) and without (A) the heavy metals removal.

and heavy metals solution) for 10 h, the changes in the crystalline structure of the MOF were insignificant. It was revealed that the Fe₃O₄@MIL-101(Cr)@PEG was quite stable in the acidic solution. Moreover, the material was stable after absorbing heavy metal ions. The obtained results indicated that the synthesized adsorbent had good structural stability and was suitable for the removal of As, Ni, Zn, Cd, and Pb ions from the *L. chuanxiong* Hort decoction.

3.5. Metal leaching rate

The metal ion leaching of the material was tested after use. The resulted leaching rate of Fe ion was 0.00016 % and that of Cr ion was 0.0049 %, indicating that Fe and Cr ions would not cause secondary pollution to *L. chuanxiong* Hort decoction.

3.6. Influence on *L. chuanxiong* Hort decoction after heavy metals removal

The quality monitoring indicators of *L. chuanxiong* Hort decoction were evaluated before and after the removal of heavy metals. In this section, the experiments of heavy metals

removal were directly carried out on the *L. chuanxiong* Hort decoction.

3.6.1. The content of Senkyunolide I, Senkyunolide A, and Ferulic acid

Since Ferulic acid and Senkyunolide are the main effective components of *L. chuanxiong* Hort, of which the pharmacological effects have been well studied (Lanlan et al., 2022; Zhen et al., 2011), Senkyunolide A, Senkyunolide I, and Ferulic acid were selected as the indicators to evaluate the influence of the adsorbent on the effective components. To evaluate the influence of the adsorption process on the active ingredients of *L. chuanxiong* Hort decoction, Senkyunolide I, Senkyunolide A, and Ferulic acid were analyzed in the same decoction with and without the removal of heavy metals. The HPLC chromatogram of Senkyunolide I, Senkyunolide A, and Ferulic acid was shown in Fig. 8.

The content of Senkyunolide I, Senkyunolide A, and Ferulic acid in the decoction of *L. chuanxiong* Hort before and after the heavy metals removal was listed in Table 5. Because the change rate was less than 8.00 %, it was clear that the content of the active ingredients was not significantly affected by the

adsorption removal process of heavy metals. The in-house fabricated adsorbent exhibited to be able to efficiently remove heavy metals in *L. chuanxiong* Hort decoction without influencing its active ingredients.

3.6.2. Solid content of the decoction

The average solid content of the solution before and after heavy metals removal was 18.19 mg·mL⁻¹ and 18.16 mg·mL⁻¹, respectively. The loss rate was only 0.16 %, indicating no obvious loss of solid content before and after removing heavy metals with the in-house fabricated adsorbent.

3.6.3. HPLC fingerprints similarity

With the same decoction, one sample solution was directly analyzed by HPLC to acquire the chromatographic fingerprint, while the other five were analyzed after the removal of heavy metals. The similarity evaluation values were all calculated to be greater than 99.9 %. Thus, there was no significant change in the number and area of the chromatographic peaks of *L. chuanxiong* decoction before and after the removal of heavy metals (Fig. 9). The consistency of the chromatogram profiles indicated that the chemical composition of the decoction remained almost complete before and after treatment. The results further verified that the in-house fabricated adsorbent would not affect the chemical components of *L. chuanxiong* decoction during the adsorption removal process of heavy metals.

4. Conclusion

In this study, a new magnetic nanomaterial (Fe₃O₄@MIL-101(Cr)@PEG) was successfully synthesized to remove heavy metals based on the PDA bridging strategy and PEG functionalization (PEG played a role in blocking the adsorption of effective components of *L. chuanxiong* Hort). The introduction of magnetism in the material allowed us to simply separate the adsorbent from the decoction of *L. chuanxiong* Hort by using an external magnetic field. The in-house fabricated adsorbent exhibited strong magnetic responsiveness, excellent hydrophilicity, and good recyclability. The kinetic and isotherm adsorption studies showed that the adsorption of these metal ions onto Fe₃O₄@MIL-101(Cr)@PEG could be described well by pseudo-second-order kinetic model as well as the Langmuir isotherm model, suggesting that the adsorption is chemisorption and monolayer. The maximum adsorption capacity of the as-prepared Fe₃O₄@MIL-101(Cr)@PEG reached 60.27 mg/g (As⁵⁺), 38.48 mg/g (Ni²⁺), 45.06 mg/g (Zn²⁺), 72.18 mg/g (Pb²⁺), and 62.29 mg/g (Cd²⁺). Thermodynamic studies revealed that the adsorption of heavy metal ions on Fe₃O₄@MIL-101(Cr)@PEG was spontaneous and exothermic within the experimental temperatures. Based on these properties, the adsorbent was verified to have good performance in the removal of Pb²⁺, Cd²⁺, As⁵⁺, Ni²⁺, and Zn²⁺ from *L. chuanxiong* decoction. In a short adsorption time, removal efficiency in the range of 51.59 %-88.19 % was obtained for the spiked heavy metals (50 µg/mL) without any significant influence on the quality of *L. chuanxiong* decoction, which was represented by the content of active ingredients, solid content, and chromatogram profile. In summary, the proposed adsorbent provided considerable removal efficiency for As⁵⁺, Cd²⁺, and Pb²⁺ and certain removal efficiency for Ni²⁺ and Zn²⁺, exhibiting great potential for heavy metals removal in medicinal herbs. Since only one kind of medicinal herb was considered, further studies are needed concerning more species of medicinal herbs and different functionalization strategies of the adsorbent.

Declaration of Competing Interest

The authors declare that they have no known competing financial interests or personal relationships that could have appeared to influence the work reported in this paper.

Acknowledgements

This work was supported by the National Natural Science Foundation of China, China (NO. 81891012, U19A2010, 82204616), National Interdisciplinary Innovation Team of Traditional Chinese Medicine, China (NO. ZYYCXTD-D-202209), Sichuan Technology Industry Innovation Team of Traditional Chinese Medicine (NO. 2022C001), Sichuan Science and Technology Program (NO. 2021JDJQ0040), China Postdoctoral Science Foundation (NO. 2019M663458), and the “Xinglin scholars” program of Chengdu University of TCM (NO. BSH2019014, QJRC2022018, XCZX2022005).

Appendix A. Supplementary material

Supplementary data to this article can be found online at <https://doi.org/10.1016/j.arabjc.2023.104635>.

References

- Abutalib, M.M., Rajeh, A., 2020. Influence of Fe₃O₄ nanoparticles on the optical, magnetic and electrical properties of PMMA/PEO composites: combined FT-IR/DFT for electrochemical applications. *J. Organomet. Chem.* 920, 121348.
- Ahmadijokani, F., Tajahmadi, S., Bahi, A., Molavi, H., Rezakazemi, M., Ko, F., Arjmand, M., 2021. Ethylenediamine-functionalized Zr-based MOF for efficient removal of heavy metal ions from water [Article]. *Chemosphere* 264, (128466–128474). <https://doi.org/10.1016/j.chemosphere.2020.128466>.
- Ahmaruzzaman, M., 2011. Industrial wastes as low-cost potential adsorbents for the treatment of wastewater laden with heavy metals. *Adv. Colloid Interface* 166 (1–2), 36–59.
- Azimi, A., Azari, A., Rezakazemi, M., Ansarpour, M., 2017. Removal of heavy metals from industrial wastewaters: a review [Review]. *ChemBioEng. Rev.* 4 (01), 37–59. <https://doi.org/10.1002/cben.201600010>.
- Bai, L., Duan, S., Jiang, W., Liu, M., Wang, S., Sang, M., Xuan, S., 2017. High performance polydopamine-functionalized mesoporous silica nanospheres for U(VI) removal [Article]. *Appl. Surf. Sci.* 426 (31), 1121–1132. <https://doi.org/10.1016/j.apsusc.2017.07.274>.
- Burtch, N.C., Jasuja, H., Walton, K.S., 2014. Water stability and adsorption in metal-organic frameworks [Review]. *Chem. Rev.* 114 (20), 10575–10612. <https://doi.org/10.1021/cr5002589>.
- Cerraholu, E., Kayan, A., Bingl, D., 2018. Multivariate optimization for removal of some heavy metals using novel inorganic-organic hybrid and calcined materials. *Sep. Sci. Technol.*, 1–10.
- Cheng, H., & Lin, Q. (2006). Study on the Adsorption Characteristics of Chitosan for Heavy Metal Residues in the Water Extract of Traditional Chinese Medicine. *Journal of Beijing Union University (Natural Sciences)*(01), 69-72. <https://doi.org/10.16255/j.cnki.ldxbz.2006.01.019>.
- Coghlan, M. L., Maker, G., Crighton, E., Haile, J., C, D., Murray, . . . Bunce, M. (2015). Combined DNA, toxicological and heavy metal analyses provides an auditing toolkit to improve pharmacovigilance of traditional Chinese medicine (TCM). *Scientific Reports*, 5, 17475, Article 17475. <https://doi.org/10.1038/srep17475>.

- Davodi, B., Jahangiri, M., & Ghorbani, M. (2019). Magnetic Fe₃O₄@polydopamine biopolymer: Synthesis, characterization and fabrication of promising nanocomposite. *Journal of Vinyl & Additive Technology*(1), 25
- Delin, Z., Rong, C., Wen, Y., Min, R., Jia, S., Min, L., 2019. Study on germlasm characteristics of four heavy metals based on different germplasm resources of Ligusticum Chuanxiong. *Chinese Med. Mater.* 42 (02), 279–284. <https://doi.org/10.13863/j.issn1001-4454.2019.02.008>.
- Duan, S., Xu, X., Liua, X., Sun, J., Hayat, T., Alsaedi, A., Li, J., 2018. Effect of Fe₃O₄@PDA morphology on the U(VI) entrapment from aqueous solution [Article]. *Appl. Surf. Sci.* 448, 297–308. <https://doi.org/10.1016/j.apsusc.2018.04.131>.
- Feng, Y., Zhu, X., & Zhang, J. (2014). Study on Heavy Metal Residues in 100 Chinese Traditional Medicine Materials. *China Pharm*, 17 (10), 1696-1697+1704.
- Fu, F., Wang, Q., 2011. Removal of heavy metal ions from wastewaters: a review [Review]. *J. Environ. Manage.* 92 (03), 407–418. <https://doi.org/10.1016/j.jenvman.2010.11.011>.
- Fuyou, F., Min, L., Zhichuan, B., 2003. Preliminary exploration on causes of contamination by heavy metals of chinese medicinal materials and measures for its improvement. *World Sci. Technol.-Modern. Traditional Chinese Med.* 5 (04).
- González, M., Pavlovic, I., Barriga, C., 2015. Cu(II), Pb(II) and Cd(II) sorption on different layered double hydroxides. a kinetic and thermodynamic study and competing factors. *Chem. Eng. J.* 269, 221–228.
- Guo, L., Zhou, L., Wnag, S., Kang, C., Hao, Q., Yang, W., Huang, L. (2017). Statistic analysis of heavy metal residues in Chinese crude drugs with the international standards of Chinese Medicine-Chinese Herbal Medicine Heavy Metal Limit. *Science and technology guide*, 35(11), 91-98.
- Guo, H., Zhang, S., North, C., Zhang, M., & Meng, X. (2020). Alkyl Thiourea Functionalised Silica for the Effective Removal of Heavy Metals from Acanthopanax senticosus Extract [Article]. *Biomed Research International*, 2020(10), 1-10, Article 9860425. <https://doi.org/10.1155/2020/9860425>.
- Han, D.H., Wang, J.P., Luo, H.L., 1994. Crystallite size effect on saturation magnetization of fine ferrimagnetic particles. *J. Magn. Magn. Mater.* 136 (1–2), 176–182.
- Hasan, Z., Khan, N.A., Jhung, S.H., 2016. Adsorptive removal of diclofenac sodium from water with Zr-based metal-organic frameworks [Article]. *Chem. Eng. J.* 284, 1406–1413. <https://doi.org/10.1016/j.cej.2015.08.087>.
- Hayati, Bagher, Mahmoodi, Niyaz, & Mohammad. (2012). Modification of activated carbon by the alkaline treatment to remove the dyes from wastewater: mechanism, isotherm and kinetic. *Desalination and water treatment: Science and engineering*, 47(1/3), 322-333
- Hupp, J.T., Poeppelmeier, K.R., 2005. Better living through nanopore chemistry. *Science* 309 (5743), 2008–2009. <https://doi.org/10.1126/science.1117808>.
- InSil, Y., JeongSook, L., SungDan, K., YunHee, K., HaeWon, P., HoeJin, R., . . . ChangGue, S. (2017). Monitoring heavy metals, residual agricultural chemicals and sulfites in traditional herbal decoctions [Article]. *Bmc Complementary and Alternative Medicine*, 17, 9, Article 154. <https://doi.org/10.1186/s12906-017-1646-y>.
- Jalayeri, H., Aprea, P., Caputo, D., Peluso, A., Pepe, F., 2020. Synthesis of amino-functionalized MIL-101(Cr) MOF for hexavalent chromium adsorption from aqueous solutions. *Environ. Nanotechnol. Monit. Manage.* 14. <https://doi.org/10.1016/j.enmm.2020.100300>.
- Jia, M., Zhu, Y., Guo, D., Bi, X., Hou, X., 2020. Surface molecularly imprinted polymer based on core-shell Fe₃O₄@ MIL-101 (Cr) for selective extraction of phenytoin sodium in plasma. *Anal. Chim. Acta* 1128, 211–220.
- Kayan, G. Ö., & Kayan, A. (2022). Polyhedral Oligomeric Silsesquioxane and Polyorganosilicon Hybrid Materials and Their Usage in the Removal of Methylene Blue Dye. 32(7), 2781–2792. - <https://doi.org/10.1007/s10904-022-02288-y>.
- Kostenko, L.S., Tomashchuk, I.I., Kovalchuk, T.V., Zaporozhets, O. A., 2019. Bentonites with grafted aminogroups: Synthesis, protolytic properties and assessing Cu(II), Cd(II) and Pb(II) adsorption capacity. *Appl. Clay Sci.* 172, 49–56.
- Kucharski, P., Bialecka, B., Śliwińska, A., & Pieprzycza, A. (2021). - Evaluation of specific capacity of poultry litter in heavy metal sorption. - 232(- 2). - <https://doi.org/10.1007/s11270-021-04984-w>.
- Lanlan, X., Xianhua, C., Ning, L., Xuezheng, L., 2022. Research progress on pharmacological action of ligusticum Senkyunolides. *Res. Pract. Modern Chinese Med.* 36 (02), 98–102. <https://doi.org/10.13728/j.1673-6427.2022.02.018>.
- Li, Z., Ma, M., Zhang, S., Zhang, Z., Zhou, L., Yun, J., Liu, R., 2020. Efficiently removal of ciprofloxacin from aqueous solution by MIL-101(Cr)-HSO₃the enhanced electrostatic interaction. *J. Porous Mater.* 27 (1), 189–204.
- Liang, X., Liang, X., 2021. Study on the excessive heavy metals in traditional Chinese Medicine. *Guangxi Trad. Chinese Med.* 44 (03), 75–77.
- Lin, A. X., Chan, G., Hu, Y., Ouyang, D., Ung, C. O. L., Shi, L., & Hu, H. (2018). Internationalization of traditional Chinese medicine: current international market, internationalization challenges and prospective suggestions. *Chinese Medicine*, 13(01), 9, Article 9. <https://doi.org/10.1186/s13020-018-0167-z>.
- Madhuri, Mandal, and, Subrata, Kundu, and, . . . and. (2005). Magnetite nanoparticles with tunable gold or silver shell. *Journal of Colloid and Interface Science*
- Mahmoodi, & Mohammad, N. (2015). Surface modification of magnetic nanoparticle and dye removal from ternary systems. *Journal of Industrial and Engineering Chemistry*, 27, 251-259
- Mendoza-Castillo, D. I., Rojas-Mayorga, C. K., García-Martínez, I. P., Pérez-Cruz, M. A., Hernández-Montoya, V., Bonilla-Petriciolet, A., & Montes-Morán, M. A. (2015). Removal of heavy metals and arsenic from aqueous solution using textile wastes from denim industry. *12(5)*, 1668. <https://doi.org/10.1007/s13762-014-0553-8>
- Mia, M. S., Yao, P., Zhu, X., Zhang, J., Xing, T., & Chen, G. (2022). Removal of heavy metals from aqueous solutions by modified waste silk [- 2022/01/29]. 92(11-12), 1965. <https://doi.org/10.1177/00405175221076026>.
- Natale, F.D., Erto, A., Lancia, A., Musmarra, D., 2008. Experimental and modelling analysis of As(V) ions adsorption on granular activated carbon. *Water Res.* 42 (8–9), 2007–2016.
- Ostolska, I., Wisniewska, M., 2017. Removal studies of Cr₂O₃ colloidal particles using cationic poly(L-lysine) and its block copolymers with poly(ethylene glycol) [Article]. *J. Mol. Liq.* 241, 952–958. <https://doi.org/10.1016/j.molliq.2017.06.100>.
- Qiu, S., Wang, Y., Wan, J., Han, J., Ma, Y., & Wang, S., 2020. Enhancing water stability of MIL-101(Cr) by doping Ni(II). *Appl. Surf. Sci.* 525, 146511.
- Saleem, H., Rafique, U., Davies, R.P., 2016. Investigations on post-synthetically modified UiO-66-NH₂ for the adsorptive removal of heavy metal ions from aqueous solution [Article]. *Micropor. Mesopor. Mater.* 221, 238–244. <https://doi.org/10.1016/j.micromeso.2015.09.043>.
- Shahabadi, N., Falsafi, M., Mansouri, K., 2016. Improving antiproliferative effect of the anticancer drug cytarabine on human promyelocytic leukemia cells by coating on Fe₃O₄@SiO₂ nanoparticles. *Colloids Surf. B Biointerfaces*, 213–222.
- Shan, R., Yan, L., Yang, K., Hao, Y., Du, B., 2015. Adsorption of Cd (II) by Mg-Al-CO₃- and magnetic Fe₃O₄/Mg-Al-CO₃-layered double hydroxides: Kinetic, isothermal, thermodynamic and mechanistic studies. *J. Hazard. Mater.* 299, 42–49. <https://doi.org/10.1016/j.jhazmat.2015.06.003>.
- Shao, M., Ning, F., Zhao, J., Wei, M., Evans, D.G., Duan, X., 2012. Preparation of Fe₃O₄@SiO₂@Layered double hydroxide core-shell microspheres for magnetic separation of proteins [Article]. *J.*

- Am. Chem. Soc. 134 (2), 1071–1077. <https://doi.org/10.1021/ja2086323>.
- Shi, Z., Xu, C., Guan, H., Li, L., Fan, L., Wang, Y., Zhang, R., 2018. Magnetic metal organic frameworks (MOFs) composite for removal of lead and malachite green in wastewater [Article]. *Colloids Surf. a-Physicochem. Eng. Asp.* 539, 382–390. <https://doi.org/10.1016/j.colsurfa.2017.12.043>.
- Shin, W. (2017). Adsorption characteristics of phenol and heavy metals on biochar from *Hizikia fusiformis*. 76(22). <https://doi.org/10.1007/s12665-017-7125-4>
- Tang, Z., Han, Q., Yu, G., Liu, F., Tan, Y., & Peng, C. (2022). Fe₃O₄@PDA/MIL-101(Cr) as magnetic solid-phase extraction sorbent for mycotoxins in licorice prior to ultrahigh-performance liquid chromatography-tandem mass spectrometry analysis. *Food Sci. Nutr.*, 10, 2224–2235. <https://doi.org/https://doi.org/10.1002/fsn3.2832>.
- Tuna, Z., A., ?zdemir, E., Simsek, E., B., . . . U. (2013). Optimization of Process Parameters for Removal of Arsenic Using Activated Carbon-Based Iron-Containing Adsorbents by Response Surface Methodology. *WATER AIR AND SOIL POLLUTION*
- Turhanen, P. A., Vepsäläinen, J. J., & Peraniemi, S. (2015). Advanced material and approach for metal ions removal from aqueous solutions [Article]. *Scientific Reports*, 5(01), 8992, Article 8992. <https://doi.org/10.1038/srep08992>.
- Vitela-Rodríguez, A.V., Rangel-Mendez, J.R., 2013. Arsenic removal by modified activated carbons with iron hydro(oxide) nanoparticles. *J. Environ. Manage.* 114 (JAN.15), 225–231.
- Wang, Y., Ye, G., Chen, H., Hu, X., Niu, Z., Ma, S., 2015. Functionalized metal-organic framework as a new platform for efficient and selective removal of cadmium(II) from aqueous solution [Article]. *J. Mater. Chem. A* 3 (29), 15292–15298. <https://doi.org/10.1039/c5ta03201f>.
- Xiong, C., Xue, C., Huang, L., Hu, P., Fan, P., Wang, S., . . . Ji, H. (2021). Enhanced selective removal of Pb(II) by modification low-cost bio-sorbent: Experiment and theoretical calculations. *Journal of Cleaner Production*, 316, 128372. <https://doi.org/https://doi.org/10.1016/j.jclepro.2021.128372>.
- Xiong, C., Xue, C., Yu, X., He, Y., Liang, Y., Zhou, X., & Ji, H. (2023). Tuning the olefin-VOCs epoxidation performance of ceria by mechanochemical loading of coinage metal. *Journal of Hazardous Materials*, 441, 129888. <https://doi.org/https://doi.org/10.1016/j.jhazmat.2022.129888>.
- Xiong, C., Wang, S., Hu, P., Huang, L., Xue, C., Yang, Z., Ji, H., 2020. Efficient selective removal of Pb(II) by using 6-aminothiouracil-modified Zr-based organic frameworks: from experiments to mechanisms. *ACS Appl. Mater. Interfaces* 12 (6), 7162–7178. <https://doi.org/10.1021/acsami.9b19516>.
- Xiong, C., Liu, H., Zhou, J., Xu, D., Liang, Y., Zhou, X., Ji, H., 2023. High selective epoxidation of 2-methylpropene over a Mo-based oxametallacycle reinforced nano composite. *Nano Res.* 16 (1), 209–218. <https://doi.org/10.1007/s12274-022-4686-7>.
- Xionghai, Y., Yitong, L., 2004. Study on residues of pesticides and heavy metals in *Ligusticum wallichii* Franch and other seven kinds of traditional Chinese Medicine. *Res. Pract. Chinese Med.* 18 (03), 7–9.
- Yalcin, G., Kayan, A., 2012. Synthesis and characterization of Zr, Ti, Al-phthalate and pyridine-2-carboxylate compounds and their use in ring opening polymerization [Article]. *Appl. Catal. a-General* 433, 223–228. <https://doi.org/10.1016/j.apcata.2012.05.019>.
- Yang, J., Hou, B., Wang, J., Tian, B., Bi, J., Wang, N., . . . Huang, X. (2019). Nanomaterials for the Removal of Heavy Metals from Wastewater. *Nanomaterials*, 9(03), 424–462, Article 424. <https://doi.org/10.3390/nano9030424>.
- Yang, C.-X., Yan, X.-P., 2011. Metal–organic framework MIL-101 (Cr) for high-performance liquid chromatographic separation of substituted aromatics. *Anal. Chem.* 83 (18), 7144–7150.
- Yanhong, Z., Minbo, L., Ying, T., 2017. Study on feasibility of selected adsorbent removing heavy metals from extracts of *salvia miltiorrhiza* Bge. *Modern Chinese Trad. Med.* 19 (03), 419–429.
- Yongdi, L., Zhonghua, L., Jianan, H., Yiyang, Z., Qin, L., 2019. Research progress on heavy metals removal from plant extracts. *Chin. Tradit. Herb. Drug* 50 (07), 1727–1733.
- Yuan, G., Tian, Y., Liu, J., Tu, H., Liao, J., Yang, J., Liu, N., 2017. Schiff base anchored on metal-organic framework for Co (II) removal from aqueous solution. *Chem. Eng. J.* 326, 691–699.
- Yufang, P., Danying, H., 2005. Effets of chitosan sorbenet on contents of heavy metal in water-extraction liquid of traditional chinese herbs. *Chem. Industry Times* 19 (11), 27–28.
- Zhang, W., He, L., & Wei, G. (2021). Research progress in detection methods of heavy metals in traditional Chinese medicine. *Scientific and technological horizon*, No.355(25), 70-72. <https://doi.org/10.19694/j.cnki.issn2095-2457.2021.25.32>
- Zhang, X., Li, S., Chen, S., Feng, F., Bai, J., Li, J., 2020. Ammoniated MOF-74(Zn) derivatives as luminescent sensor for highly selective detection of tetrabromobisphenol A [Article]. *Ecotoxicol. Environ. Saf.* 187., <https://doi.org/10.1016/j.ecoenv.2019.109821> 109821.
- Zhang, X., Wang, X., Qiu, H., Sun, X., Han, M., Guo, Y., 2020. Nanoadsorbents preparing from oligoethylene glycol dendron and citric acid: enhanced adsorption effect for the removal of heavy metal ions [Article]. *Colloids Surf. B-Biointerfaces* 189., <https://doi.org/10.1016/j.colsurfb.2020.110876> 110876.
- Zhang, X., Yan, L., Li, J., Yu, H., 2020. Adsorption of heavy metals by L-cysteine intercalated layered double hydroxide: kinetic, isothermal and mechanistic studies [Article]. *J. Colloid Interface Sci.* 562, 149–158. <https://doi.org/10.1016/j.jcis.2019.12.028>.
- Zhang, M., Zhang, X., He, X., Chen, L., Zhang, Y., 2012. A self-assembled polydopamine film on the surface of magnetic nanoparticles for specific capture of protein [Article]. *Nanoscale* 4 (10), 3141–3147. <https://doi.org/10.1039/c2nr30316g>.
- Zhao, Z., Li, J., Wen, T., Shen, C., Wang, X., Xu, A., 2015. Surface functionalization graphene oxide by polydopamine for high affinity of radionuclides [Article]. *Colloids Surf. a-Physicochem. Eng. Asp.* 482, 258–266. <https://doi.org/10.1016/j.colsurfa.2015.05.020>.
- Zhen, W., Xinyong, L., Jing, W., Hongfei, C., Chenchen, M., 2011. Research progress on pharmacological effects of Ligustrazine and ferulic acid compounds. *Qilu Pharm.* 30 (11), 665–667.
- Zheng, F., Wang, C., Huang, K., Li, J., 2021. Surface adsorption in PEG/hydroxyapatite and PEG/Dickite composite phase change materials. *Energy Fuel* 35 (13), 10850–10859.
- Zhou, H., Long, J.R., Yaghi, O.M., 2012. Introduction to metal-organic frameworks [Editorial Material]. *Chem. Rev.* 112 (02), 673–674. <https://doi.org/10.1021/cr300014x>.